JLAB-THY-TBD
SLAC-PUB-TBD

Gluon matter distribution in the proton and pion from extended holographic light-front QCD

Guy F. de Téramond,[1] H. G. Dosch,[2] Tianbo Liu,[3,*]
Raza Sabbir Sufian,[4,5,†] Stanley J. Brodsky,[6] and Alexandre Deur[5]
(HLFHS Collaboration)

[1] Laboratorio de Física Teórica y Computacional, Universidad de Costa Rica, 11501 San José, Costa Rica
[2] Institut für Theoretische Physik der Universität, D-69120 Heidelberg, Germany
[3] Key Laboratory of Particle Physics and Particle Irradiation (MOE), Institute of Frontier and Interdisciplinary Science, Shandong University, Qingdao, Shandong 266237, China
[4] Department of Physics, William & Mary, Williamsburg, Virginia 23187, USA
[5] Thomas Jefferson National Accelerator Facility, Newport News, VA 23606, USA
[6] SLAC National Accelerator Laboratory, Stanford University, Stanford, CA 94309, USA

The holographic light-front QCD framework provides a unified nonperturbative description of the hadron mass spectrum, form factors and quark distributions. In this article we extend holographic QCD in order to describe the gluonic distribution in both the proton and pion from the coupling of the metric fluctuations induced by the spin-two Pomeron with the energy momentum tensor in anti-de Sitter space, together with constraints imposed by the Veneziano model without additional free parameters. The gluonic and quark distributions are shown to have significantly different effective QCD scales.

Introduction.— The gluonic composition of hadrons plays a key role in understanding the confining phase of quantum chromodynamics (QCD), which is still an unresolved issue in modern particle physics. A key nonperturbative feature of color-confining hadron dynamics is the intrinsic gluon distribution which exists in hadrons over a time scale independent of the resolution of the external probe. The coupling of the rank-two energy-momentum tensor (EMT), the tensor which couples to gravity [1–3], provide fundamental constraints on the quark and gluon generalized parton distribution functions (GPDs) of a hadron [4–6]. Gravitational form factors (GFFs), the hadronic matrix elements of the EMT, describe the coupling of a hadron to the graviton and thus provide information on the dynamics of quarks and gluons within hadrons due to the internal shear forces and pressure distributions of the quarks and gluons [7–9]. In this letter, we present an extended holographic light-front QCD framework for studying the gluon GFFs and provide predictions for the intrinsic gluon distributions of hadrons without introducing additional parameters.

In addition to the role of gluons as fundamental constituents and as the glue that binds the quarks into hadrons, the knowledge of gluon distributions within hadrons is also essential for the understanding of the Higgs boson production [10] and particle production cross sections at small-momentum fraction x. The near threshold production of heavy vector quarkonium [11], such as the J/ψ and Υ, is dominated by the gluon EMT: It is expected to shed light on the QCD scale anomaly at the origin of the proton mass [12]. On the other hand, the intrinsic gluon parton distribution function (PDF) of the pion is of particular theoretical interest for understanding nonperturbative aspects of QCD, such as its dual nature as the lightest QCD bound state, but also as a Goldstone mode associated with the spontaneous breaking of chiral symmetry. Because of the special role of the pion in QCD, there have been sustained efforts and proposals to explore its gluon distribution [13], along with that of the nucleon, one of the main goals of the upcoming Electron-Ion-Collider (EIC) [14, 15].

Holographic light-front QCD (HLFQCD), a nonperturbative framework based on the gauge/gravity correspondence [16] and its light-front (LF) holographic mapping [17–19], has the remarkable feature that it reproduces, within its expected precision, the hadronic spectra with the minimal number of parameters: the confining scale λ and effective quark masses. The LF holographic framework is compatible with chiral symmetry breaking, related in this formalism to the confinement dynamics [20], and with superconformal quantum mechanics [21–23], which leads to unexpected connections across the full hadron spectrum [24]. It reproduces the structure of hadronic spectra as predicted by dual models, most prominently the Veneziano model [25] with its typical features: linear Regge trajectories with a universal slope and the existence of "daughter trajectories".

The form factors (FFs) obtained within the HLFQCD framework can be expressed by Euler-Beta functions [26, 27], a feature also predicted by the generalized Veneziano model [28, 29], which includes the electromagnetic (EM) current and the FFs: $F_{\rm EM}(t) \sim B\left(\gamma, 1-\alpha_\rho(t)\right)$, where $\alpha_\rho(t)$ is trajectory of the ρ-vector-meson, coupling to the quark current in the hadron. We emphasize that, within HLFQCD, the parameter γ, related to the fall-off of the EM FF at large momentum transfer t, is not arbitrary, but fixed by the twist structure of the Fock state, $\gamma = \tau - 1$, consistent with the exclusive counting rules [30, 31]: The twist τ is the number of constituents N, $\tau = N$ ($\tau = N + L$ for LF orbital angular momentum L).

The form of the quark distributions in the hadrons is heavily constrained by the analytic representation of the FFs. Furthermore, very natural assumptions, such as the incorporation of the inclusive-exclusive relation at large longitudinal momentum fraction x [32], allowed us to predict, in a very satisfactory way, the quark distributions in mesons and nucleons [26, 33], as well as the strange-antistrange and the charm-anticharm asymmetries [34, 35] in the nucleon. Notably, the preliminary NNPDF4.1 global analysis [36] indicates a valence-like intrinsic charm contribution $|uudc\bar{c}\rangle$ in the nucleon, consistent with the intrinsic charm-anticharm asymmetry computed in [35]. Similarly, the $|uudg\rangle$ and $|u\bar{d}g\rangle$ Fock states should provide the leading contributions to the intrinsic gluon distributions in the proton and the pion.

In this letter we extend our previous framework by incorporating gluonic matter with significantly different quarkonic and gluonic scales. Several models for non-perturbative QCD, see e.g. [37], predict that the static potential between quarks, $V_{\bar{q}q}$, and that between gluons, V_{gg}, are substantially different, and scale with N_C like the quadratic Casimir operator between the fundamental and adjoint representations, $\frac{V_{gg}}{V_{\bar{q}q}} \sim \frac{2N_C^2}{N_C^2-1}$. The Casimir scaling between loops is confirmed by lattice calculation [38] and is in qualitative accordance with the smaller slope of the Pomeron as compared to the Reggeons, $\alpha_P \ll \alpha_\rho$. It is therefore natural to adopt different scales λ_q and λ_g for quarkonic and gluonic matter with $\lambda_g \gg \lambda_q$.

We study the perturbation of the anti-de Sitter (AdS) metric by an external spin-two current which couples to the EMT in the bulk: It allows us to identify the tensor Pomeron in the physical boundary space with the induced metric fluctuations in AdS, and thus to determine the infrared deformation of the AdS metrics for the gluon content in terms of the Pomeron slope. It determines within the present approach, not only the scale of the gluonic matter, but also an opposite-sign dilaton for the gluonic sector. By further imposing the structure of the generalized Veneziano amplitudes for a spin-two current, we are able to relate the different scales appearing in the problem and extend the relation between FFs and GPDs [4–6] found in [26], without introducing additional free parameters.

Pomeron exchange and gravitational form factors.— As pointed out in [39], soft interactions play an important role in high-energy collisions. Especially, the trajectory for diffractive processes, the Pomeron, has a dominant role at small-angle high-energy scattering, which is beyond the applicability of perturbative QCD. Since the early days of QCD, Pomeron exchange was associated with two (or more) gluons [40–42]. The Pomeron couples as a rank-two tensor to hadrons [43–47] and couples strongly to gluons. It remains unclear whether there exists a relation between the soft [48] and hard [49–51] Pomerons and their cross-over regime. It may be sufficient to consider only the soft Pomeron if one looks into the intrinsic gluon component of the nucleon structure functions, except, perhaps, for extremely small-x [49–53]. Therefore we use the soft Pomeron of Donnachie and Landshoff [48] with the effective Regge trajectory

$$\alpha_P(t) = \alpha_P(0) + \alpha'_P t, \tag{1}$$

which is interpreted in QCD as a $J^{PC} = 2^{++}$, bound state of two gluons with intercept $\alpha_P(0) \simeq 1.0808$, and slope $\alpha'_P \simeq 0.25\,\mathrm{GeV}^{-2}$ [39]. In contrast, the hard Pomeron has an intercept ~ 1.34. Using the gauge/gravity duality [16], Pomeron exchange is identified as the graviton of the dual AdS theory [54–58] and the first hadronic state on the Pomeron trajectory should be a 2^{++} glueball [59].

We consider the perturbation of the AdS gravity action by an arbitrary external source at the AdS asymptotic boundary which propagates inside AdS space and couples to the EMT [60, 61]. By performing a deformation of the AdS metrics $ds^2 = g_{MN}dx^M dx^N$ about its AdS background, $g_{MN} \to g_{MN} + h_{MN}$, we obtain the effective action $S_{\text{eff}}[h,\Phi] = S_g[h] + S_i[h,\Phi]$ in the string frame with 5-dimensional coordinates $x^M = (x^\mu, z)$

$$S_g[h] = -\tfrac{1}{4}\int d^5x\sqrt{g}\, e^{\varphi_g(z)}\big(\partial_L h^{MN}\partial^L h_{MN} - \tfrac{1}{2}\partial_L h\,\partial^L h\big), \tag{2}$$

$$S_i[h,\Phi] = \tfrac{1}{2}\int d^5x\sqrt{g}\, h_{MN}T^{MN}, \tag{3}$$

where we use the harmonic gauge $\partial_L h^L_M = \frac{1}{2}\partial_M h$, $h \equiv h^L_L$, to obtain (2). The interaction term (3) represents the coupling of the matter fields EMT with the graviton probe in AdS –which we identify here with the Pomeron. To simplify the discussion we represent the hadron matter content by a scalar field Φ with action

$$S_q[\Phi] = \int d^5x\sqrt{g}e^{\varphi_q(z)}\big(g^{MN}\partial_M\Phi^*\partial_N\Phi - \mu^2\Phi^*\Phi\big)\,; \tag{4}$$

It describes a pion with AdS mass $(\mu R)^2 = 4$ for the lowest state (R is the AdS radius), thus the total effective action $S_{\text{eff}}[h,\Phi] = S_g[h] + S_q[\Phi] + S_i[h,\Phi]$. From the holographic point of view the field Φ represents the full hadron with mass $P_\mu P^\mu = M^2$, which couples to gravity without distinction between its quark and gluon constituents. The EMT for the matter field follows from (4), $T_{MN} = \partial_M\Phi^*\partial_N\Phi + \partial_N\Phi^*\partial_M\Phi$, therefore the transition amplitude for the EMT in (3) is

$$\int d^4x\,dz\sqrt{g}\,h_{\mu\nu}\left(\partial^\mu\Phi^*_{P'}\partial^\nu\Phi_P + \partial^\nu\Phi^*_{P'}\partial^\mu\Phi_P\right), \tag{5}$$

with $\Phi_P(x,z) = e^{-iP\cdot x}\Phi(z)$, $\quad P_\mu P^\mu = P'_\mu P'^\mu = M^2$.

We choose the harmonic-traceless gauge $\partial_L h^L_M = \frac{1}{2}\partial_M h = 0$ and consider the propagation of the gravitational fluctuation h_{MN} with components along Minkowski coordinates $h_{zz} = h_{z\mu} = 0$. From (2) we obtain the linearized Einstein equation

$$-\frac{z^3}{e^{\varphi_g(z)}}\partial_z\left(\frac{e^{\varphi_g(z)}}{z^3}\partial_z h_\mu^{\ \nu}\right) + \partial_\rho\partial^\rho h_\mu^{\ \nu} = 0, \tag{6}$$

where $h_{\mu\nu}$ couples to the transverse and traceless part of the EMT in (3). The boundary limit of the graviton probe is a plane wave along the physical coordinates with polarization indices along the transverse directions $h_\mu^\nu(x, z \to 0) = \epsilon_\mu^\nu e^{-iq\cdot x}$, where $q^2 = -Q^2 < 0$. We thus write $h_\mu^\nu(x,z) = \epsilon_\mu^\nu e^{-iq\cdot x} H(q^2, z)$, with $H(q^2 = 0, z) = H(q^2, z = 0) = 1$. For a soft-wall profile $\varphi_g(z) = -\lambda_g z^2$ [62] the solution to (6) is given by

$$\begin{aligned} H(a,\xi) &= \Gamma\,(2+a)\,U\,(a,-1,\xi) \\ &= a\,(2+a)\,\int_0^1 dx\, x^{a-1}(1-x)e^{-\xi x(1-x)}, \end{aligned} \tag{7}$$

where $a = Q^2/4\lambda_g$, $\xi = \lambda_g z^2$, and $U(a, b, z)$ is the Tricomi confluent hypergeometric function.

The usual expression of the GFF from the hadronic matrix elements of the EMT

$$\left\langle P' \left| T_\mu^{\ \nu} \right| P \right\rangle = \left(P^\nu P'_\mu + P_\mu P'^\nu\right) A(Q^2), \tag{8}$$

follows from extracting the delta function from momentum conservation in (5). We obtain for $A(Q^2)$ [60, 61]

$$A_\tau(Q^2) = \int \frac{dz}{z^3}\, H(Q^2, z)\Phi_\tau^2(z), \tag{9}$$

with $A_\tau(0) = 1$. Upon substituting in (9) the x-integral representation of the bulk-to-boundary propagator (7) and the AdS twist-τ hadron bound-state solution [19], $\Phi_\tau(z) \sim z^\tau e^{-\lambda_q z^2/2}$, we find

$$\begin{aligned} A_\tau(Q^2) = \tau(\tau-1)B\,(\tau-1, 2+a) \\ {}_2F_1\,(a, \tau-1; \tau+1+a; r)\,, \end{aligned} \tag{10}$$

where ${}_2F_1(a, b; c; z)$ is the Gauss hypergeometric function and $r = 1 - \lambda_g/\lambda_q$. The quark component of the action $S_q[\Phi]$ (4) is modified by an exponential dilaton term $e^{\varphi_q(z)} = e^{\lambda_q z^2}$ with $\lambda_q = 1/4\alpha'_\rho \simeq (0.5\,\mathrm{GeV})^2$, specific to the light front mapping to physical $3 + 1$ dimensional space in HLFQCD [19] and the constraints imposed by the superconformal algebraic structure [24]. The "gluonic component" $S_g[h]$ (2) is not constrained by additional symmetries and is modified by $e^{\varphi_g(z)} = e^{-\lambda_g z^2}$ with $\lambda_g = 1/4\alpha'_P \simeq 1\,\mathrm{GeV}^2$, from the Pomeron slope. The interaction term $S_i[h, \Phi]$ (3) has no deformation term and does not introduce an additional scale.

The GFF given by (10) does not possess analytic continuation between the space-like, $q^2 < 0$, and time-like, $q^2 > 0$ domains; in fact, the hypergeometric function ${}_2F_1$ in (10) grows monotonically for $q^2 > 0$ yielding unphysical results. This problem can be overcome, however, by noticing that the physical scale in the interaction term (3) is determined by the Pomeron scale which interacts with the small components of a high virtuality hadron over a distance $\sim 1/\sqrt{\alpha_P}$, meaning that, effectively, the scales λ_g and λ_q become comparable in the interaction term, making the ratio r in (10) to vanish. Noticing that ${}_2F_1(a, b; c; 0) = 1$ we are led to

$$A_\tau(Q^2) = \frac{1}{N_\tau} B\left(\tau-1, 2-\alpha_P(Q^2)\right), \tag{11}$$

with $N_\tau = B\,(\tau-1, 2-\alpha_P(0))$, the result of the generalized Veneziano model [25, 28, 29] for a spin-two current. Alternatively, if we impose the structure of the Veneziano amplitude we can relate the different scales appearing in the interaction term, and, by writing (11), we have extended the holographic results for zero Regge intercept, to arbitrary Regge trajectories, and in particular to the spin-two Pomeron trajectory.

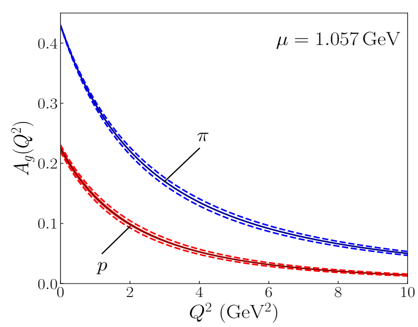

FIG. 1. Gluon gravitational form factor $A_g(Q^2)$ of the proton (red) and the pion (blue). The dashed curves indicate the uncertainty from the variation of λ_g by $\pm 5\%$.

For integer twist the GFF (11) can be expressed as a product of $\tau - 1$ time-like poles located at

$$-Q^2 = M_n^2 = \frac{1}{\alpha'_P}\left(n + 2 - \alpha_P(0)\right), \tag{12}$$

the radial excitation spectrum of the spin-2 exchanged particles in the leading $C = +$ Pomeron trajectory (1). The lowest state in this trajectory, the 2^{++}, has the mass $M \simeq 1.92$ GeV, compared with the lattice results of about 2.3 GeV [39, 63, 64]: The lowest mass glueball 0^{++} lie on a daughter trajectory. The predictions for the GFF, $A_g(Q^2)$, for the nucleon and pion are presented in Fig. 1. We find for the gluon mass radius

$$\langle r_g^2 \rangle = \frac{6}{A_g(0)} \frac{dA_g(t)}{dt}\Big|_{t=0}, \tag{13}$$

$\langle r_g^2 \rangle_p = 2.93/\lambda_g = (0.34\,\mathrm{fm})^2$ and $\langle r_g^2 \rangle_\pi = 2.41/\lambda_g = (0.31\,\mathrm{fm})^2$ for the proton and pion, indicating a gluon-mass distribution concentrated in a rather small region compared with the spread of the charge [39], and also smaller than the proton mass radius found in [60, 65–67]. The normalization used in Fig. 1 is discussed below.

Gluon distribution functions.— Recent calculations of the gluon distribution functions in the nucleon have been performed using holographic approaches, such as in [68–71]. Following the unified approach advanced in [26, 33] we determine in the present work the unpolarized gluon distributions in the nucleon and pion without introducing any additional free parameters. In the nonperturbative domain, low virtuality gluons interact strongly with each other to generate the color confinement potential so that one cannot distinguish individual gluon quanta. At higher virtualities constituent gluons appear as new degrees of freedom. The lowest gluonic Fock state of the proton is $|qqqg\rangle$ and, for simplicity, we consider this Fock state to be the dominant contribution to the intrinsic gluon distribution.

Using (11) and the integral representation of the Beta function, the gravitational form factor $A_\tau(t)$ can be written in the reparametrization invariant form

$$A_\tau(t) = \frac{1}{N_\tau}\int_0^1 dx\, w'(x) w(x)^{1-\alpha(t)}\big[1 - w(x)\big]^{\tau-2}, \quad (14)$$

provided that $w(x)$ satisfies the constraints $w(0) = 0$, $w(1) = 1$ and $w'(x) \geq 0$.

The GFF can also be expressed as the first moment of the integrated expression of the gluon GPD at zero skewness, $H^g_\tau(x,t) \equiv H^g_\tau(x, \xi = 0, t)$,

$$\begin{aligned} A^g_\tau(t) &= \int_0^1 x\, dx H^g_\tau(x,t) \\ &= \int_0^1 x\, dx\, g_\tau(x) \exp[t f(x)], \end{aligned} \quad (15)$$

where $f(x)$ is the profile function and $g_\tau(x)$ is the collinear gluon PDF of twist-τ. Comparing (15) with the holographic expression (14) we find that both functions, $f(x)$ and $g_\tau(x)$, are determined in terms of the reparametrization function, $w(x)$, by

$$f_g(x) = \alpha'_P \log\Big(\frac{1}{w(x)}\Big), \quad (16)$$

$$g_\tau(x) = \frac{1}{N_\tau}\frac{w'(x)}{x}[1 - w(x)]^{\tau-2} w(x)^{1-\alpha_P(0)}, \quad (17)$$

where $g_\tau(x)$ is normalized by $\int_0^1 dx\, g_\tau(x) = 1$

If we identify x with the hadron LF momentum fraction, physical constraints on $w(x)$ are imposed at small and large-x [72]: At $x \to 0$, $w(x) \sim x$ from Regge theory [73], and at $x \to 1$ from the inclusive-exclusive counting rule [32], $g_\tau(x) \sim (1-x)^{2\tau-3}$, which fixes $w'(1) = 0$. The leading $(1-x)$-exponent determined in [74] by fitting the NNPDF gluon distribution [75] is consistent with the large-x counting rule.

The gluon distribution of the proton can be expressed as the sum of contributions from all Fock states,

$$g(x) = \sum_\tau c_\tau g_\tau(x), \quad (18)$$

where the coefficients, c_τ, represent the probability of each Fock component. In practice, one has to apply a truncation up to some value of τ. In this study we only keep the leading term, $\tau = 4$, and determine the coefficient $c_\tau = 4$ using the momentum sum rule

$$\int_0^1 dx\, x\big[g(x) + \sum_q q(x)\big] = 1, \quad (19)$$

where q runs over all quark flavors. It also corresponds to the sum rule of the helicity-conserving GFF $A(t)$, $A^g(0) + \sum_q A^q(0) = 1$, which is a measure of the momentum fraction carried by each constituent. Similarly the helicity-flip GFF $B^q(t)$ provides a measure of the orbital angular momentum carried by each constituent of a hadron at $t = 0$ and it is at the origin of Ji's sum rule [5]. The constraint $B^g(0) + \sum_q B^q(0) = 0$ was originally derived from the equivalence principle [76] and can be formally derived Fock state by Fock state in LF quantization [77].

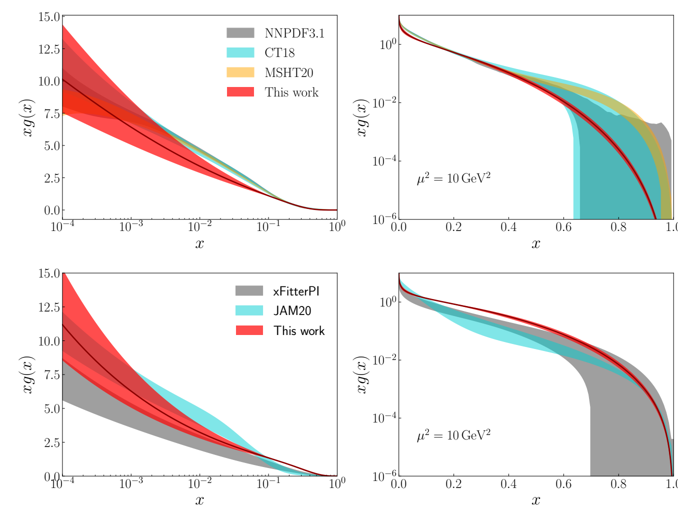

FIG. 2. Unpolarized gluon distribution in the proton (top panel) and pion (bottom panel) from HLFQCD and comparison with PDFs' global fits. The figures on left and right are the same distributions with different scales for $xg(x)$ and x to enhance the view of the small and large-x regions respectively.

Taking the quark distributions and the reparametrization function $w(x)$ from Ref. [33], $w(x) = x^{1-x}\exp[-0.480(1-x)^2]$, we determine $c_{\tau=4} = 0.225 \pm 0.006$ and thus the distribution at the input scale $\mu_0 = 1.057\,\mathrm{GeV}$. Together with the quark distributions, we evolve the gluon distribution to $\mu^2 = 10\,\mathrm{GeV}^2$. The model results are compared in Fig. 2 with global analyses of gluon PDFs of the nucleon [75, 78, 79]. Contributions from higher Fock states are expected to be suppressed at large x, and may affect the overall normalization through the momentum sum rule: Higher Fock states will tend to suppress the distribution at large x while enhancing the distribution at small x.

Incorporating the universality of our approach, we now compute the gluon distribution in the pion. Similar to the case of the proton, we only consider the lowest $\tau = 3$ Fock state $|u\bar{d}g\rangle$ with one constituent gluon. The coupling of the Pomeron to the hadrons depends on the vertex, but the trajectory $\alpha_P(t)$ (1) is the same and unique to the Pomeron. Considering the valence quark distributions determined in Ref. [26], $|\pi\rangle = 0.875\,|u\bar{d}\rangle + 0.125\,|u\bar{d}q\bar{q}\rangle$, we express the total quark distribution as $q_\pi(x) \equiv q_u(x) + q_d(x) + q_{\bar{u}}(x) + q_{\bar{d}}(x) \simeq 1.75\,q_{\tau=2}(x) + 0.5\,q_{\tau=4}(x)$. Using the momentum sum rule we obtain the gluon distribution of the pion as $g_\pi(x) = 0.429\,g_{\tau=3}(x)$. We show in Fig. 2 the results evolved to $\mu^2 = 10\,\mathrm{GeV}^2$ and a comparison is made with global analyses [80, 81]. We note that the overall normalization of the gluon distribution from our calculation seems overestimated in comparison with some recent global analyses, which may arise from neglecting higher Fock states for the gluon GFF.

Conclusion and outlook.— The light-front holographic extension presented in this article allows us to describe the intrinsic gluon distributions in the proton and pion from the coupling of the spin-two Pomeron trajectory: This extension leads to the holographic description of gluonic matter in the proton and pion with vastly different effective scales. The comparison of the gluon distributions, after DGLAP evolution, between our theoretical predictions and global analyses clearly demonstrates the predictive power of this new framework and paves the way for an extension of our results for the gravitational form factor $A(t)$ to the other two GFFs $B(t)$ and $C(t)$ [3]. Of particular relevance is the coupling of the scalar Pomeron trajectory –with the same Pomeron slope, but different intercept, to compute the form factor $C(t)$ [67, 68]. It will allow us to describe, with enough precision, the distribution of internal shear forces and pressure inside the proton and therefore its dynamical stability.

Acknowledgments. RSS thanks Patrick Barry for providing the JAM20 gluon distribution of the pion. TL is supported in part by National Natural Science Foundation of China under Contract No. 11775118. RSS is supported by U.S. DOE grant No. DE-FG02-04ER41302 and in part by the U.S. Department of Energy contract No. DE-AC05-06OR23177, under which Jefferson Science Associates, LLC, manages and operates Jefferson Lab.

* liutb@sdu.edu.cn
† sufian@jlab.org

[1] I. Y. Kobzarev and L. B. Okun, Gravitational interaction of fermions, Zh. Eksp. Teor. Fiz. **43**, 1904-1909 (1962).
[2] S. Weinberg, Photons and gravitons in S-matrix theory: Derivation of charge conservation and equality of gravitational and inertial mass, Phys. Rev. **135**, B1049-B1056 (1964).
[3] H. Pagels, Energy-momentum structure form factors of particles, Phys. Rev. **144**, 1250-1260 (1966).
[4] D. Müller, D. Robaschik, B. Geyer, F. M. Dittes and J. Hořejši, Wave functions, evolution equations and evolution kernels from light-ray operators of QCD, Fortsch. Phys. **42**, 101-141 (1994), [arXiv:hep-ph/9812448 [hep-ph]].
[5] X. D. Ji, Gauge-invariant decomposition of nucleon spin, Phys. Rev. Lett. **78**, 610 (1997), [arXiv:hep-ph/9603249].
[6] A. V. Radyushkin, Nonforward parton distributions, Phys. Rev. D **56**, 5524 (1997), [arXiv:hep-ph/9704207 [hep-ph]].
[7] M. V. Polyakov, Generalized parton distributions and strong forces inside nucleons and nuclei, Phys. Lett. B **555**, 57-62 (2003), [arXiv:hep-ph/0210165 [hep-ph]].
[8] M. V. Polyakov and P. Schweitzer, Forces inside hadrons: pressure, surface tension, mechanical radius, and all that, Int. J. Mod. Phys. A **33**, no.26, 1830025 (2018), [arXiv:1805.06596 [hep-ph]].
[9] V. D. Burkert, L. Elouadrhiri and F. X. Girod, The pressure distribution inside the proton, Nature **557**, no. 7705, 396-399 (2018).
[10] H. M. Georgi, S. L. Glashow, M. E. Machacek and D. V. Nanopoulos, Higgs bosons from two-gluon annihilation in proton-proton collisions, Phys. Rev. Lett. **40**, 692 (1978).
[11] S. J. Brodsky, E. Chudakov, P. Hoyer and J. M. Laget, Photoproduction of charm near threshold, Phys. Lett. B **498**, 23-28 (2001), [arXiv:hep-ph/0010343 [hep-ph]].
[12] D. Kharzeev, H. Satz, A. Syamtomov and G. Zinovjev, J/ψ photoproduction and the gluon structure of the nucleon, Eur. Phys. J. C **9**, 459-462 (1999), [arXiv:hep-ph/9901375 [hep-ph]].
[13] A. C. Aguilar, Z. Ahmed, C. Aidala, S. Ali, V. Andrieux, J. Arrington, A. Bashir, V. Berdnikov, D. Binosi and L. Chang, *et al.*, Pion and kaon structure at the electron-ion collider, Eur. Phys. J. A **55**, no.10, 190 (2019), [arXiv:1907.08218 [nucl-ex]].
[14] A. Accardi *et al.*, Electron Ion Collider: The next QCD frontier, Eur. Phys. J. A **52**, no.9, 268 (2016), [arXiv:1212.1701 [nucl-ex]].
[15] R. Abdul Khalek, A. Accardi, J. Adam, D. Adamiak, W. Akers, M. Albaladejo, A. Al-bataineh, M. G. Alexeev, F. Ameli and P. Antonioli, *et al.*, Science requirements and detector concepts for the Electron-Ion Collider: EIC Yellow Report, [arXiv:2103.05419 [physics.ins-det]].
[16] J. M. Maldacena, The large-N limit of superconformal field theories and supergravity, Int. J. Theor. Phys. **38**, 1113 (1999) [Adv. Theor. Math. Phys. **2**, 231 (1998)], [arXiv:hep-th/9711200 [hep-th]].
[17] S. J. Brodsky and G. F. de Téramond, Hadronic spectra

and light-front wave functions in holographic QCD, Phys. Rev. Lett. **96**, 201601 (2006), [arXiv:hep-ph/0602252].
[18] G. F. de Téramond and S. J. Brodsky, Light-front holography: A first approximation to QCD, Phys. Rev. Lett. **102**, 081601 (2009), [arXiv:0809.4899 [hep-ph]].
[19] S. J. Brodsky, G. F. de Téramond, H. G. Dosch and J. Erlich, Light-front holographic QCD and emerging confinement, Phys. Rept. **584** (2015), 1-105, [arXiv:1407.8131 [hep-ph]].
[20] G. F. de Téramond and S. J. Brodsky, Longitudinal dynamics and chiral symmetry breaking in holographic light-front QCD, [arXiv:2103.10950 [hep-ph]].
[21] S. Fubini and E. Rabinovici, Superconformal quantum mechanics, Nucl. Phys. B **245**, 17 (1984).
[22] G. F. de Téramond, H. G. Dosch and S. J. Brodsky, Baryon spectrum from superconformal quantum mechanics and its light-front holographic embedding, Phys. Rev. D **91**, 045040 (2015), [arXiv:1411.5243 [hep-ph]].
[23] H. G. Dosch, G. F. de Téramond and S. J. Brodsky, Superconformal baryon-meson symmetry and light-front holographic QCD, Phys. Rev. D **91**, 085016 (2015), [arXiv:1501.00959 [hep-th]].
[24] S. J. Brodsky, G. F. de Téramond and H. G. Dosch, Light-front holography and supersymmetric conformal algebra: A novel approach to hadron spectroscopy, structure, and dynamics, [arXiv:2004.07756 [hep-ph]].
[25] G. Veneziano, Construction of a crossing-symmetric, Regge-behaved amplitude for linearly rising trajectories, Nuovo Cim. A **57**, 190 (1968).
[26] G. F. de Téramond, T. Liu, R. S. Sufian, H. G. Dosch, S. J. Brodsky, and A. Deur Universality of generalized parton distributions in light-front holographic QCD, Phys. Rev. Lett. **120**, no.18, 182001 (2018), [arXiv:1801.09154 [hep-ph]].
[27] L. Zou and H. G. Dosch, A very practical guide to light-front holographic QCD, [arXiv:1801.00607 [hep-ph]].
[28] M. Ademollo and E. Del Giudice, Nonstrong amplitudes in a Veneziano-type model, Nuovo Cim. A **63**, 639 (1969).
[29] P. V. Landshoff and J. C. Polkinghorne, The scaling law for deep inelastic scattering in a new Veneziano-like amplitude, Nucl. Phys. B **19**, 432 (1970).
[30] S. J. Brodsky and G. R. Farrar, Scaling laws at large transverse momentum, Phys. Rev. Lett. **31**, 1153 (1973);
[31] V. A. Matveev, R. M. Muradian and A. N. Tavkhelidze, Automodellism in the large-angle elastic scattering and structure of hadrons, Lett. Nuovo Cim. **7**, 719 (1973).
[32] S. D. Drell and T. M. Yan, Connection of elastic electromagnetic nucleon form-factors at large Q^2 and deep inelastic structure functions near threshold, Phys. Rev. Lett. **24**, 181 (1970).
[33] T. Liu, R. S. Sufian, G. F. de Téramond, H. G. Dosch, S. J. Brodsky, and A. Deur, Unified description of polarized and unpolarized quark distributions in the proton, Phys. Rev. Lett. **124**, no.8, 082003 (2020), [arXiv:1909.13818 [hep-ph]].
[34] R. S. Sufian, T. Liu, G. F. de Téramond, H. G. Dosch, S. J. Brodsky, A. Deur, M. T. Islam and B.-Q. Ma, Nonperturbative strange-quark sea from lattice QCD, light-front holography, and meson-baryon fluctuation models, Phys. Rev. D **98**, 114004 (2018), [arXiv:1809.04975 [hep-ph]].
[35] R. S. Sufian, T. Liu, A. Alexandru, S. J. Brodsky, G. F. de Téramond, H. G. Dosch, T. Draper, K.-F. Liu and Y.-B. Yang, Constraints on charm-anticharm asymmetry in the nucleon from lattice QCD, Phys. Lett. B **808**, 135633 (2020), [arXiv:2003.01078 [hep-lat]].
[36] J. Rojo, Progress in the NNPDF global analyses of proton structure, [arXiv:2104.09174 [hep-ph]].
[37] A. Di Giacomo, H. G. Dosch, V. I. Shevchenko and Y. A. Simonov, Field correlators in QCD: Theory and applications, Phys. Rep. **372**, 319-368 (2002), [arXiv:hep-ph/0007223 [hep-ph]].
[38] G. S. Bali, Casimir scaling of SU(3) static potentials, Phys. Rev. D **62**, 114503 (2000), [arXiv:hep-lat/0006022 [hep-lat]].
[39] P. A. Zyla *et al.* (Particle Data Group), Review of Particle Physics, Prog. Theo. Exp. Phys. **2020**, no.8, 083C01 (2020).
[40] L. V. Gribov, E. M. Levin and M. G. Ryskin, Semihard processes in QCD, Phys. Rep. **100**, 1-150 (1983).
[41] B. Badelek, M. Krawczyk, K. Charchula and J. Kwiecinski, Small-x physics in deep-inelastic lepton-hadron scattering, Rev. Mod. Phys. **64**, 927-960 (1992).
[42] S. Donnachie, H. G. Dosch, O. Nachtmann and P. Landshoff, Pomeron physics and QCD, Camb. Monogr. Part. Phys. Nucl. Phys. Cosmol. **19**, 1-347 (2002).
[43] L. Adamczyk *et al.* (STAR Collaboration), Single spin asymmetry A_N in polarized proton-proton elastic scattering at $\sqrt{s} = 200$ GeV, Phys. Lett. B **719**, 62-69 (2013), [arXiv:1206.1928 [nucl-ex]].
[44] C. Ewerz, M. Maniatis and O. Nachtmann, A model for soft high-energy scattering: Tensor pomeron and vector odderon, Annals Phys. **342**, 31-77 (2014), [arXiv:1309.3478 [hep-ph]].
[45] C. Ewerz, P. Lebiedowicz, O. Nachtmann and A. Szczurek, Helicity in proton–proton elastic scattering and the spin structure of the Pomeron, Phys. Lett. B **763**, 382-387 (2016), [arXiv:1606.08067 [hep-ph]].
[46] P. Lebiedowicz, O. Nachtmann and A. Szczurek, Exclusive diffractive production of $\pi^+\pi^-\pi^+\pi^-$ via the intermediate $\sigma\sigma$ and $\rho\rho$ states in proton-proton collisions within tensor Pomeron approach, Phys. Rev. D **94**, no. 3, 034017 (2016), [arXiv:1606.05126 [hep-ph]].
[47] D. Britzger, C. Ewerz, S. Glazov, O. Nachtmann and S. Schmitt, The tensor Pomeron and low-x deep inelastic scattering, Phys. Rev. D **100**, no.11, 114007 (2019), [arXiv:1901.08524 [hep-ph]].
[48] A. Donnachie and P. V. Landshoff, Total cross-sections, Phys. Lett. B **296**, 227-232 (1992), [arXiv:hep-ph/9209205 [hep-ph]].
[49] E. A. Kuraev, L. N. Lipatov, and V. S. Fadin, The Pomeranchuk singularity in nonabelian gauge theories, Sov. Phys. JETP **45**, 199-204 (1977).
[50] I. I. Balitsky and L. N. Lipatov, The Pomeranchuk singularity in quantum chromodynamics, Sov. J. Nucl. Phys. **28**, 822-829 (1978).
[51] R. Kirschner and L. N. Lipatov, Double logarithmic asymptotics and Regge singularities of quark amplitudes with flavour exchange, Nucl. Phys. B **213**, 122-148 (1983).
[52] A. H. Mueller and J. W. Qiu, Gluon recombination and shadowing at small values of x, Nucl. Phys. B **268**, 427-452 (1986).
[53] Y. V. Kovchegov, Small-x F_2 structure function of a nucleus including multiple pomeron exchanges, Phys. Rev. D **60**, 034008 (1999).
[54] R. C. Brower, J. Polchinski, M. J. Strassler and C. I. Tan, The Pomeron and gauge/string duality, JHEP **12**, 005

(2007), [arXiv:hep-th/0603115 [hep-th]].

[55] L. Cornalba and M. S. Costa, Saturation in deep inelastic scattering from AdS/CFT, Phys. Rev. D **78**, 096010 (2008), [arXiv:0804.1562 [hep-ph]].

[56] S. K. Domokos, J. A. Harvey and N. Mann, The Pomeron contribution to pp and $p\bar{p}$ scattering in AdS/QCD, Phys. Rev. D **80**, 126015 (2009), [arXiv:0907.1084 [hep-ph]].

[57] R. C. Brower, M. Djuric, I. Sarcevic and C. I. Tan, String-gauge dual description of deep inelastic scattering at small-x, J. High Energy Phys. 11 (2010) 051, [arXiv:1007.2259 [hep-ph]].

[58] M. S. Costa and M. Djuric, Deeply virtual Compton scattering from gauge/gravity duality, Phys. Rev. D **86**, 016009 (2012), [arXiv:1201.1307 [hep-th]].

[59] There exist many computations of glueballs in top-down holographic models, see for example, C. Csaki, H. Ooguri, Y. Oz and J. Terning, Glueball mass spectrum from supergravity, J. High Energy Phys. 01 (1999) 017, [arXiv:hep-th/9806021 [hep-th]], and also in bottom-up models starting from H. Boschi-Filho, N. R. F. Braga and H. L. Carrion, Glueball Regge trajectories from gauge-string duality and the Pomeron, Phys. Rev. D **73**, 047901 (2006), [arXiv:hep-th/0507063 [hep-th]]. For a recent computation, see for example, M. Rinaldi and V. Vento, Meson and glueball spectroscopy within the graviton soft wall model, [arXiv:2101.02616 [hep-ph]], and references therein.

[60] Z. Abidin and C. E. Carlson, Gravitational form factors of vector mesons in an AdS/QCD model, Phys. Rev. D **77**, 095007 (2008), [arXiv:0801.3839 [hep-ph]]; Nucleon electromagnetic and gravitational form factors from holography, Phys. Rev. D **79**, 115003 (2009), [arXiv:0903.4818 [hep-ph]].

[61] S. J. Brodsky and G. F. de Téramond, Light-front dynamics and AdS/QCD correspondence: Gravitational form factors of composite hadrons, Phys. Rev. D **78**, 025032 (2008), [arXiv:0804.0452 [hep-ph]].

[62] A. Karch, E. Katz, D. T. Son and M. A. Stephanov, Linear confinement and AdS/QCD, Phys. Rev. D **74**, 015005 (2006), [arXiv:hep-ph/0602229 [hep-ph]].

[63] C. J. Morningstar and M. J. Peardon, Glueball spectrum from an anisotropic lattice study, Phys. Rev. D **60**, 034509 (1999), [arXiv:hep-lat/9901004 [hep-lat]].

[64] H. B. Meyer and M. J. Teper, Glueball Regge trajectories and the Pomeron: A Lattice study, Phys. Lett. B **605**, 344-354 (2005), [arXiv:hep-ph/0409183 [hep-ph]].

[65] Y. Guo, X. Ji and Y. Liu, QCD analysis of near-threshold photon-proton production of heavy quarkonium, Phys. Rev. D **103**, no.9, 096010 (2021), [arXiv:2103.11506 [hep-ph]].

[66] D. E. Kharzeev, The mass radius of the proton, [arXiv:2102.00110 [hep-ph]].

[67] K. A. Mamo and I. Zahed, Nucleon mass radii and distribution: Holographic QCD, Lattice QCD and GlueX data, Phys. Rev. D **103**, no.9, 094010 (2021), [arXiv:2103.03186 [hep-ph]].

[68] K. A. Mamo and I. Zahed, Diffractive photoproduction of J/ψ and Υ using holographic QCD: gravitational form factors and GPD of gluons in the proton, Phys. Rev. D **101**, no.8, 086003 (2020), [arXiv:1910.04707 [hep-ph]].

[69] A. Watanabe, T. Sawada and M. Huang, Extraction of gluon distributions from structure functions at small x in holographic QCD, Phys. Lett. B **805**, 135470 (2020), [arXiv:1910.10008 [hep-ph]].

[70] V. E. Lyubovitskij and I. Schmidt, Gluon parton densities in soft-wall AdS/QCD, Phys. Rev. D **103**, 094017 (2021), [arXiv:2012.01334 [hep-ph]].

[71] J. Lan, K. Fu, C. Mondal, X. Zhao and j. P. Vary, Light mesons with one dynamical gluon on the light front, [arXiv:2106.04954 [hep-ph]].

[72] R. D. Ball, E. R. Nocera and J. Rojo, The asymptotic behaviour of parton distributions at small and large x, Eur. Phys. J. C **76**, no.7, 383 (2016), [arXiv:1604.00024 [hep-ph]].

[73] T. Regge, Introduction to complex orbital momenta, Nuovo Cim. **14**, 951 (1959).

[74] R. S. Sufian, T. Liu and A. Paul, Gluon distributions and their applications to Ioffe-time distributions, Phys. Rev. D **103**, no.3, 036007 (2021), [arXiv:2012.01532 [hep-ph]].

[75] R. D. Ball *et al.* (NNPDF Collaboration), Parton distributions from high-precision collider data, Eur. Phys. J. C **77**, no.10, 663 (2017), [arXiv:1604.00024 [hep-ph]].

[76] O. V. Teryaev, Spin structure of nucleon and equivalence principle, [arXiv:hep-ph/9904376 [hep-ph]].

[77] S. J. Brodsky, D. S. Hwang, B.-Q. Ma and I. Schmidt, Light-cone representation of the spin and orbital angular momentum of relativistic composite systems, Nucl. Phys. B **593**, 311-335 (2001), [arXiv:hep-th/0003082 [hep-th]].

[78] T. J. Hou, J. Gao, T. J. Hobbs, K. Xie, S. Dulat, M. Guzzi, J. Huston, P. Nadolsky, J. Pumplin and C. Schmidt, *et al.* New CTEQ global analysis of quantum chromodynamics with high-precision data from the LHC, Phys. Rev. D **103**, no.1, 014013 (2021), [arXiv:1912.10053 [hep-ph]].

[79] S. Bailey, T. Cridge, L. A. Harland-Lang, A. D. Martin and R. S. Thorne, Parton distributions from LHC, HERA, Tevatron and fixed target data: MSHT20 PDFs, Eur. Phys. J. C **81**, no.4, 341 (2021), [arXiv:2012.04684 [hep-ph]].

[80] I. Novikov, H. Abdolmaleki, D. Britzger, A. Cooper-Sarkar, F. Giuli, A. Glazov, A. Kusina, A. Luszczak, F. Olness and P. Starovoitov, *et al.* Parton distribution functions of the charged pion within the xFitter framework, Phys. Rev. D **102**, no.1, 014040 (2020), [arXiv:2002.02902 [hep-ph]].

[81] N. Y. Cao *et al.* (JAM Collaboration), Towards the three-dimensional parton structure of the pion: Integrating transverse momentum data into global QCD analysis, Phys. Rev. D **103**, no.11, 114014 (2021), [arXiv:2103.02159 [hep-ph]].